Genet. Res., Camb. (2007), **89**, *pp.* 27–38. © 2007 Cambridge University Press
doi:10.1017/S0016672307008622 Printed in the United Kingdom

Functional mapping of reaction norms to multiple environmental signals

JIASHENG WU[1], YANRU ZENG[2], JIANQING HUANG[2], WEI HOU[3], JUN ZHU[1] AND RONGLING WU[2,3]*

[1] *College of Agriculture and Biotechnology, Zhejiang University, Hangzhou, Zhejiang 310029, People's Republic of China*
[2] *School of Forestry and Biotechnology, Zhejiang Forestry University, Lin'an, Zhejiang 311300, People's Republic of China*
[3] *Department of Statistics, University of Florida, Gainesville, FL 32611, USA*

(*Received 5 August 2006; and in revised form 31 January 2007*)

Summary

Whether there are different genes involved in response to different environmental signals and how these genes interact to determine the final expression of the trait are of fundamental importance in agricultural and biological research. We present a statistical framework for mapping environment-induced genes (or quantitative trait loci, QTLs) of major effects on the expression of a trait that respond to changing environments. This framework is constructed with a maximum-likelihood-based mixture model, in which the mean and covariance structure of environment-induced responses is modelled. The means for responses to continuous environmental states, referred to as reaction norms, are approximated for different QTL genotypes by mathematical equations that were derived from fundamental biological principles or based on statistical goodness-of-fit to observational data. The residual covariance between different environmental states was modelled by autoregressive processes. Such an approach to studying the genetic control of reaction norms can be expected to be advantageous over traditional mapping approaches in which no biological principles and statistical structures are considered. We demonstrate the analytical procedure and power of this approach by modelling the photosynthetic rate process as a function of temperature and light irradiance. Our approach allows for testing how a QTL affects the reaction norm of photosynthetic rate to a specific environment and whether there exist different QTLs to mediate photosynthetic responses to temperature and light irradiance, respectively.

1. Introduction

The study of genetic and developmental interactions that modulate an organism's response to environmental signals has become one of the most vital areas in environmental genomic, evolutionary genomic and toxicogenomic research (Lynch & Walsh, 1998; Borlak, 2005). To increase the efficiency of breeding programmes seeking high-yielding genotypes adapted to a wide range of environments, we need to gain knowledge about the genetic basis of structural-functional relationships that regulate plant or animal form and size (Cronk, 2005). Genetic control mechanisms for developmental aspects of an organism are being synthesized into evolutionary biology. Whereas a conceptual framework for *evo-devo* has emerged to integrate evolution and development (Raff, 2000; Arthur, 2002), biologists are creating *eco-devo* to emphasize environmental influences on the development of organisms (Dusheck, 2002; Sultan, 2005).

The question of how genetic, developmental and environmental factors are coordinated to direct biological processes has been poorly understood. This is partly due to a lack of effective analytical tools that can handle intrinsically complicated relationships among these factors. The phenotypes of most biological traits involve multiple quantitative trait loci (QTLs) (Lander & Botstein, 1989), with varying effects and each segregating in the Mendelian fashion, whose expression relies upon the stage of development and the environmental condition in which the

* Corresponding author. Department of Statistics, University of Florida, Gainesville, FL 32611, USA. Telephone.: +1 (352) 3923806. Fax: +1 (352) 3928555. e-mail: rwu@stat.ufl.edu

organism is reared. Thus, any analytical approach that attempts to estimate the specific effects of individual development- or environment-dependent QTLs should consider the coordinating mechanisms that govern the dynamic changes of a living system.

Ptak & Schaeffer (1993) developed test-day models for the genetic analysis of milk yield as a function of days from calving. These models were further extended to consider the inheritance of major genes (Lund *et al*., 2002). Some sophisticated models based on random regression have been developed to model multiple traits and multiple environmental factors (Kolmodin *et al*., 2002). These studies have used statistically convenient mathematical functions, but the elucidation of the relationship between genetic control and development using *biologically relevant* mathematical functions has not been explored thoroughly until the publication of *functional mapping*, originally by R. Wu and colleagues (Ma *et al*., 2002; Wu *et al*., 2003*a*, *b*, 2004*a–c*; reviewed in Wu & Lin, 2006). The basic rationale of functional mapping is to bridge gene actions and interactions of the underlying QTL within developmental pathways by parametric or non-parametric models. Through reducing the number of parameters to be estimated, functional mapping displays increased statistical power and stability.

From a statistical standpoint, functional mapping strives to jointly model mean and covariance structures for a longitudinal trait. However, unlike general treatments of longitudinal problems (Pourahmadi, 1999; Pan & Mackenzie, 2003; Wu & Pourahmadi, 2003), functional mapping integrates the parameter estimation and test process within a mixture-based likelihood framework. By embedding the mathematical aspects of biological principles, such as growth equations (von Bertalanffy, 1957; Richards, 1959; West *et al*., 2001), into the estimation process of QTL parameters, functional mapping might be biologically more relevant than traditional mapping models that fail to consider biology. The results derived from functional mapping can be expected to be closer to biological reality.

The principle of functional mapping can be used to study the genetic architecture of environmentally sensitive phenotypic variation for a complex trait. Phenotypic responsiveness of a genotype to different environmental signals is known as phenotypic plasticity (Via *et al*., 1995). The genetic mapping of phenotypic plasticity over discrete environments can be performed by traditional statistical approaches, such as multivariate mapping (Jiang & Zeng, 1995), through incorporating the environment-dependent genetic effects into the mapping model. However, these approaches can only analyse a limited number of discrete environments. Phenotypic plasticity over continuous environmental gradients, such as temperature and relative humidity gradients, also called *reaction norms*, are regarded as 'infinite-dimensional traits' that require an infinite number of measurements to be completely described (Kirkpatrick & Heckman, 1989; Gomulkiewicz & Kirkpatrick, 1992). Statistical models for analysing the genetic control of reaction norms should take into account their infinite-dimensional feature. Understanding the variation, selection and evolution of continuous reaction norms has been a central challenge for evolutionary ecology for several decades (Stearns, 1989; Scheiner, 1993; Schlichting & Pigliucci, 1998; Wu, 1998; Sultan, 2000, 2003*a*, *b*, 2004).

In this article, we will develop a functional-mapping-based model to map QTLs that control continuous reaction norms for a quantitative trait to multiple different environments. The new model for multivariate reaction norms will be constructed within a maximum-likelihood-based mixture framework, in which the means for reaction norms are modelled for different QTL genotypes by biologically meaningful mathematical equations and the residual covariance between different environmental states is modelled by autoregressive processes. We formulate a series of hypothesis tests regarding the pattern of the genetic control for reaction norms to various environmental stimuli. Simulation studies have been conducted to investigate the statistical properties of the new model.

2. Multivariate reaction norms

The development of complex traits is the consequence of interactions among a multitude of genetic and environmental factors that affect trait development. This process is inherently complicated, but can be illustrated by a landscape of phenotype formed by genetic and environmental variables. Here, we used a diagram drawn by Wolf (2002) to elucidate this landscape (Fig. 1). The surface of the landscape defines the phenotype determined by a particular combination of underlying genetic (such as additive, dominant or epistatic) and environmental factors (such as temperature, light or moisture) that interact with each other through complex molecular and developmental mechanisms. The number of underlying factors contributing to phenotypic variation is equivalent to the number of dimensions of the landscape space. As Wolf (2002) pointed out, the number of underlying factors can be unlimited, implying that a landscape can exist in hyperspace, i.e., very-high-dimensional space. In Fig. 1, the phenotype of an individual is determined by the values of two underlying factors. By characterizing the topographical features of such landscape, a fundamental question of how each underlying factor contributes to the expression of a particular trait individually or

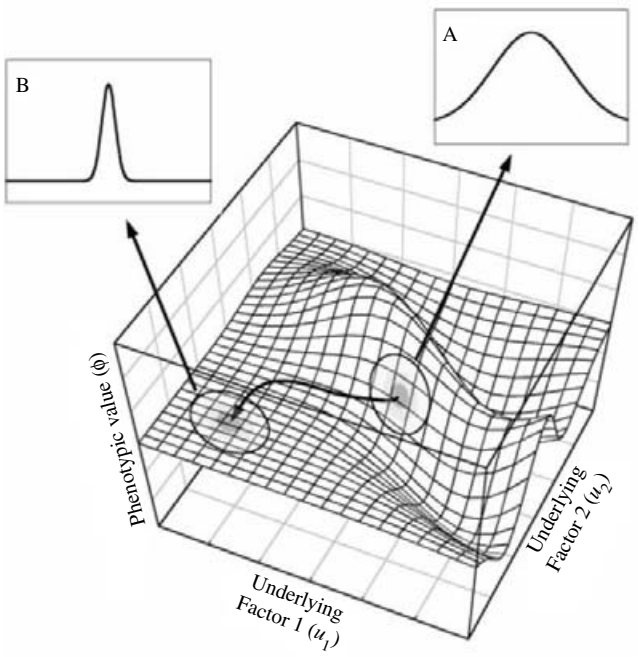

Fig. 1. A graphic representation of the formation of a phenotype by a landscape. The phenotypic formation is a function of the value of underlying factors 1 and 2 (u_1 and u_2) that interact during trait development. Two shaded ovals represent two different areas on the surface, one being flatter (pointing to inset A) and the second being steeper (pointing to inset B). The steeper one is associated with a dramatic change in phenotypic expression contributed by a small change in the underlying factors (indicated by the distribution in inset B), whereas the flatter one is associated with a different pattern in which dramatic changes in the underlying factors lead to only a minor change in phenotypic expression (indicated by the distribution in inset A). Adapted from Wolf (2002).

interactively can be addressed. These features typically include 'slope', 'curvature', 'peak-valley' and 'ridge' (Wolf, 2002). A similar description of the topography can also be applied to hyperdimensional landscapes, although the intuitive interpretation of the features become increasingly difficult with increased dimensionality.

As demonstrated in a series of developmental studies of insects (Davidowitz *et al.*, 2003, 2004; Davidowitz & Nijhout, 2004), the degree and pattern of phenotypic sensitivities to different environmental stimuli may be controlled by the same or different genetic systems. This should be common also in other organisms. For example, photosynthesis as the primary process in plant growth is determined by many biotic or abiotic environmental factors, such as leaf age, carbon dioxide concentration, temperature, irradiance, nutrient and water potential. The responsiveness of photosynthetic rate to each of these factors follows different physiological mechanisms. A major challenge is how to determine the genetic background of the reaction norms of photosynthetic rate to these factors simultaneously. Mechanistic or empirical models have been proposed to describe the relationship of various biotic or abiotic factors, separately or jointly, with photosynthetic rate (Wu, 1993). These models can be embedded into the functional mapping of dynamic traits to reveal specific QTLs for environmental sensitivity.

For simplicity, our functional-mapping-based model is constructed to map photosynthetic sensitivities to temperature and irradiance. A typical mathematical function, the non-rectangular hyperbola, has been developed to describe the relationship of photosynthetic rate (P) with leaf irradiance (I) and temperature (T), expressed as (Thornley & Johnson, 1990)

$$P(I,T)=\frac{1}{2\theta}\left\{\alpha I+P_m-\sqrt{(\alpha I+P_m)^2-4\theta\alpha IP_m}\right\}, \quad (1)$$

where θ is the fraction of the resistance of carbon dioxide diffusion over the sum of diffusion and carboxylation resistances, with $0<\theta<1$, α is the photochemical efficiency and P_m is the maximum photosynthetic rate at a saturating irradiance, which is determined by temperature in a linear function:

$$P_m=\begin{cases}P_m(20)\left(\dfrac{T-T^*}{20-T^*}\right) & T\geqslant T^*(2)\\ 0 & T<T^*\end{cases}. \quad (2)$$

$P_m(20)$ is the value of P_m at the reference temperature of 20 °C and T^* is the reference temperature for the

start-up of photosynthesis, i.e. the temperature at which photosynthesis ceases. The choice of T^* should be based on a good fit to observed data over a temperature range. Fig. 2 shows the reaction norms of photosynthetic rate over irradiance and temperature. By estimating the parameters (α, $P_m(20)$, θ) contained in equations (1) and (2), we can determine in which pattern changes in irradiance and temperature cause the alteration in photosynthetic rate.

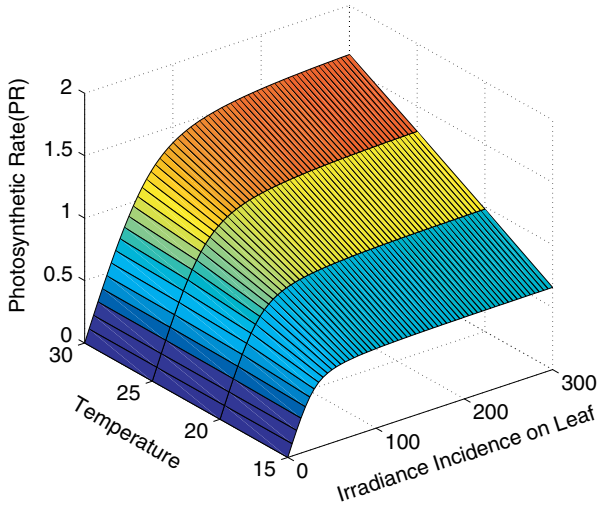

Fig. 2. Non-rectangular hyperbola describing photosynthetic rate as a function of irradiance and temperature. The parameters of photosynthetic rate used to draw the landscape are (α, $P_m(20)$, θ) = (0·02,1,0·9) obtained from published literature (Thornley & Johnson, 1990).

3. Functional mapping model

(i) *Likelihood*

Our analysis and modelling will be based on a simple backcross design. Extensions to other more complicated designs are straightforward. Consider a backcross population composed of n plants, in which photosynthetic rate is measured at a series of irradiance ($s_1 = 1, \ldots, S_1$) and temperature levels ($s_2 = 1, \ldots, S_2$). Each backcross progeny is genotyped for molecular markers to construct a genetic linkage map. Suppose there are two QTLs, each with two genotypes 1 and 2, that affect the reaction norms of photosynthetic rate to irradiance and temperature. These two QTLs that have four possible genotypes, generally labelled by $j_1 j_2$ ($j_1, j_2 = 1, 2$), in the backcross family should be located on the genetic map and can be inferred by the markers that constructed the map. The likelihood of phenotypic ($\mathbf{y}$) and marker data ($\mathbf{M}$) at the QTL is written, within the mixture model context, as

$$L(\Theta_l, \mathbf{u}, \Sigma | \mathbf{y}, \mathbf{M}) = \prod_{i=1}^{n} \left[\sum_{j_1=1}^{2} \sum_{j_2=1}^{2} \omega_{j_1 j_2 | i} f_{j_1 j_2}(\mathbf{y}_i) \right] \qquad (3)$$

where $\omega_{j_1 j_2 | i}$ is the conditional probability of a QTL genotype given marker information for backcross i, which contains the location parameters of the QTL (Θ_l), and $f_{j_1 j_2}(\mathbf{y}_i)$ is a multivariate normal distribution of phenotypic vector

$$\mathbf{y}_i = [\underbrace{y_i(1,1), \ldots, y_i(1,S_2)}_{\text{irradiance } 1}, \ldots, \underbrace{y_i(S_1,1), \ldots, y_i(S_1,S_2)}_{\text{irradiance } S_1}]$$

with QTL genotype-specific mean vector

$$\mathbf{u}_{j_1 j_2} = [\underbrace{u_{j_1 j_2}(1,1), \ldots, u_{j_1 j_2}(1,S_2)}_{\text{irradiance } 1}, \ldots, \underbrace{u_{j_1 j_2}(S_1,1), \ldots, u_{j_1 j_2}(S_1,S_2)}_{\text{irradiance } S_1}],$$

arrayed by $\mathbf{u} = \{\mathbf{u}_{j_1 j_2}\}_{j_1, j_2 = 1}^{2}$, and residual covariance matrix Σ.

(ii) *Modelling the mean vector and residual covariance matrix*

According to the idea of functional mapping (Ma *et al.*, 2002), we will use the mathematical function of photosynthetic rate (equations 1 and 2) to model the mean vector, the element of which is expressed as

$$u_{j_1 j_2}(s_1, s_2) = \frac{1}{2\theta_{j_1 j_2}} \left\{ \alpha_{j_1 j_2} s_1 + P_{m j_1 j_2} - \sqrt{(\alpha_{j_1 j_2} s_1 + P_{m j_1 j_2})^2 - 4\theta_{j_1 j_2} \alpha_{j_1 j_2} s_1 P_{m j_1 j_2}} \right\}, \quad j_1, j_2 = 1, 2$$

$$P_{m j_1 j_2} = \begin{cases} P_{m j_1 j_2}(20) \left(\dfrac{s_2 - T^*}{20 - T^*} \right) & s_2 \geqslant T^* \\ 0 & s_2 < T^* \end{cases}$$

Parameters $(\alpha_{j_1 j_2}, \theta_{j_1 j_2}, P_{m j_1 j_2}(20))$, symbolized by $\Theta_{u_{j_1 j_2}}$, describe the shape of the reaction norms of photosynthetic rate for a QTL genotype across different irradiance and temperature levels. The residual covariance matrix Σ for the two-dimensional reaction norms can be modelled as a completely separable structure (Porcu *et al.*, 2006, 2007), in which Σ is obtained as the Kronecker product of two covariance matrices each for a reaction norm process, i.e.

$$\Sigma = \Sigma_1 \otimes \Sigma_2 \qquad (4)$$

where Σ_1 and Σ_2 are the $(S_1 \times S_2)$ and $(S_2 \times S_2)$ covariance matrices among different temperatures and different irradiance levels, respectively. This separable

approach has computational advantages (Porcu *et al*., 2006*a*, *b*), although it does not take into account the interactions between the two different reaction norm processes.

The structure of the two covariance matrices in equation (4) can be modelled by a stationary autoregressive (AR) (Diggle *et al*., 2002) or non-stationary antedependence (SAD) process (Gabriel, 1962). According to these two processes, the residual at the current state can be described by a weighted sum of its preceding values and a white noise error. The number of the preceding states that have a direct effect on the current residual is defined as the order (r), with the process expressed as AR(r) or SAD(r). For AR(1), the residual variance is expressed as $\sigma_1^2(1) = \ldots = \sigma_1^2(S_1) = \sigma_1^2$ for Σ_1 and $\sigma_2^2(1) = \ldots = \sigma_2^2(S_2) = \sigma_2^2$ for Σ_2, whereas the correlation decays only with state lag in an autoregressive coefficient ρ_1 and ρ_2 for Σ_1 and Σ_2, respectively. The variance and covariance stationarity assumptions of the AR process can be relaxed in the SAD process. By defining an antedependence parameter, ϕ_1 and ϕ_2, and an innovative variance, v_1^2 and v_2^2, for Σ_1 and Σ_2, respectively, SAD(1) allows the variance and covariance to be non-stationary (Núñez-Antón *et al*., 1999; Zimmerman & Núñez-Antón, 2001). We use Θ_v to denote these covariance-modelling parameters for AR or SAD. The advantage of using AR and SAD to model the covariance structures lies in the explicit forms of the determinants and inverses of the covariance matrices (Ma *et al*., 2002; Zhao *et al*., 2005*a*), which facilitates the estimation process of unknown parameters.

Ma *et al*. (2002) and Wu *et al*. (2004*b*) implemented the EM algorithm to obtain the maximum likelihood estinates (MLEs) of unknown parameters, $\Theta = (\Theta_l, \{\Theta_{u_{j_1 j_2}}\}_{j_1=1,\ j_2=1}^{2,2}, \Theta_v)$, for functional mapping described by the likelihood (3). To increase the computing efficiency of functional mapping, the simplex and Newton-Raphson algorithms can be coupled in the estimation process with the EM algorithm (Zhao *et al*., 2004). A computer program for computational algorithms used in this study is available from the authors.

(iii) *Hypothesis testing*

After the MLEs of the unknown parameters are obtained, a number of hypotheses can be tested within the functional mapping framework (Wu *et al*., 2004*a*). The existence of QTLs that determine the shape of reaction curves can be tested by formulating the null hypothesis

$$\Theta_{u_{j_1 j_2}} \equiv \Theta_{\bar{u}}, \quad \text{for all } j_1, j_2 = 1, 2, \tag{5}$$

which states that all individual curves can be fitted with a mean curve by parameters $\Theta_{\bar{u}} = (\alpha, \theta, P_m(20))$. The log-likelihood ratio between this null hypothesis and its alternative is calculated and then compared against the critical threshold determined from permutation tests to test the significance of the QTL detected. The additive effects of each QTL and additive × additive epistatic effects between the two QTL on reaction norms can be further tested using a procedure described in Wu *et al*. (2004*a*).

An alternative to testing the existence of QTLs for reaction norms is based on the volume under surface (V) expressed as the integral of the photosynthetic reaction norm function over both irradiance and temperature, with the corresponding null hypothesis

$$V_{j_1 j_2} \equiv V, \quad \text{for all } j_1, j_2 = 1, 2. \tag{6}$$

where

$$V_{j_1 j_2} = \int_1^{S_1} \int_1^{S_2} P(s_1, s_2) ds_1 ds_2.$$

The functional-mapping-incorporated model allows for separate tests of the genetic control of the reaction norm to different environmental factors. While equations (1) and (2) describe the joint effects of irradiance and temperature on photosynthetic rate, the marginal effect of each of these two environmental factors is expressed as an integral, i.e.

$$P(s_1) = \int_1^{S_2} P(s_1, s_2) ds_2,$$

and

$$P(s_2) = \int_1^{S_1} P(s_1, s_2) ds_1,$$

for the irradiance and temperature reaction norms, respectively. The null hypotheses for testing the separate effect of the QTLs on temperature- and irradiance-dependent reaction norms are formulated, respectively, as

$$P_{j_1 j_2}(s_1) \equiv P(s_1), \quad \text{for all } j_1, j_2 = 1, 2 \tag{7}$$

and

$$P_{j_1 j_2}(s_2) \equiv P(s_2), \quad \text{for all } j_1, j_2 = 1, 2. \tag{8}$$

Whether the QTLs affect the interaction effects between irradiance and temperature on photosynthetic rate can also be tested by formulating the null hypothesis expressed as

$$\Delta_{j_1 j_2} = P_{j_1 j_2}(s_1, s_2) - P_{j_1 j_2}(s_1) - P_{j_1 j_2}(s_2) + V_{j_1 j_2} \equiv \Delta, \quad \text{for all } j_1, j_2 = 1, 2. \tag{9}$$

It should be noted that hypotheses (6) and (9) are different in terms of the pattern of QTL control. All four hypotheses can be extended to test the effects of different genetic components, additive and additive × additive, on two-dimensional reaction norms.

The slope of reaction norm with the change in an environmental factor can be calculated by differentiating the photosynthetic process with respect to this environmental factor, whereas the gradient of reaction norm is expressed as the partial derivative of the photosynthetic process with both environmental factors. How the QTL affects the slope and gradient of reaction norms can be tested by formulating the following null hypotheses:

$$d_{j_1 j_2}(s_1) \equiv d(s_1), \quad \text{for all } j_1, j_2 = 1, 2 \tag{10}$$

for irradiance,

$$d_{j_1 j_2}(s_2) \equiv d(s_2), \quad \text{for all } j_1, j_2 = 1, 2 \tag{11}$$

for temperature, and

$$\delta_{j_1 j_2} \equiv d_{j_1 j_2}(s_1, s_2) - d_{j_1 j_2}(s_1) - d_{j_1 j_2}(s_2) + d_{j_1 j_2} \equiv \delta, \quad \text{for all } j_1, j_2 = 1, 2 \tag{12}$$

for both the environmental factors, with

$$d_{j_1 j_2}(s_1) = \frac{\partial}{\partial s_1} P(s_1, s_2),$$

$$d_{j_1 j_2}(s_2) = \frac{\partial}{\partial s_2} P(s_1, s_2),$$

$$d_{j_1 j_2}(s_1, s_2) = \frac{\partial^2}{\partial s_1 \partial s_2} P(s_1, s_2).$$

The integrals and differentiations of photosynthetic reaction norms used for the above hypotheses are derived in the Appendix.

4. Monte Carlo simulation

(i) *Design*

Simulation studies were performed to investigate the statistical flexibility, stability and power of the model. We simulated a backcross of different sizes ($n = 100$ and 400) in which a 100 cM long linkage group composed of 11 evenly spaced markers was generated. In the first setting, one QTL was hypothesized to be located 46 cM from the first marker of the linkage group. Two genotypes at the hypothesized QTL, which are assigned different combinations of photosynthetic rate parameters ($\theta_{j_1 j_2}, \alpha_{j_1 j_2}, P_{mj_1 j_2}(20)$), form two different surfaces in the irradiance–temperature space. Fig. 2 illustrates such a photosynthetic surface for a typical QTL genotype. The phenotypic value for a given irradiance (0, 50, 100, 200, 300) and temperature (15, 20, 25, 30) was simulated by summing the genotypic values and residual errors which follow a multivariate normal distribution with mean vector **0** and covariance matrix Σ (equation 4). The structure of Σ is modelled by AR(1). The constant variance σ^2 was determined by assuming different heritability (H^2) levels, 0·1 and 0·4, at a representative state for irradiance and temperature. In the second setting, we performed simulations under a two-QTL model, in which two QTLs, forming four backcross genotypes, were assumed at 46 and 73 cM from the first marker of the linkage group.

(ii) *Results*

In general, our model was robust in that the locations of QTLs and their values for reaction norms were accurately and precisely estimated. Tables 1 and 2 tabulate such estimation results from one representative parameter space under different sample sizes and heritability levels. For the backcross with a modest sample size (100) and heritability (0·1), surface parameters for two QTL genotypes under the one-QTL model and the parameters that model residual covariance matrices can be estimated with reasonable accuracy and precision (Table 1). The estimation precision increases monotonically with increased sample size and heritability. In the case of two QTLs, all the parameters can still be estimated, but the estimation precision is greatly reduced compared with the one-QTL model because of the larger number of unknowns being estimated. Reasonable estimation precision for the two-QTL model can be achieved when sample size and heritability increase to 400 and 0·4, respectively (Table 2). But the three curve parameters respond to sample size and heritability differently in estimation precision, with α being more sensitive than P_m and θ. For the two-QTL model, the QTL positions can be well estimated. Fig. 3 is an example of the log-likelihood ratio (LR) profile for a sample size 400 and heritability 0·1 across two dimensions of chromosomal lengths, with the LR peak being broadly consistent with the true QTL positions.

Theoretically, hypotheses (6)–(12) can each be used to test the pattern of QTL control over reaction norms for any data set, although it is computationally expensive. Here, we used one random simulation data set to test the effect of the two QTLs on the surface of photosynthetic reaction norms based on hypothesis (6). The log-likelihood ratio tests for the additive effects of two QTLs and their additive × additive effect for the volume under surface were estimated, respectively, suggesting that they are all significant compared with the critical thresholds determined from simulation studies.

5. Discussion

As naturally occurring environmental variation, such as temperature and irradiance, can be continuous, so can the response or sensitivity of an organism to the change in environment. The genetic and developmental basis of continuous environmental sensitivity

Table 1. *The means of the MLEs of the QTL position and the parameters that model photosynthetic reaction norm processes for two different QTL genotypes* (*Qq and qq*) *for one hypothesized QTL Q and residual covariance matrices for 100 simulation replicates. The square roots of the mean squared errors of the MLEs are given in parentheses*

			Qq			Qq					
H^2	n	Position (46)	$\alpha_1 = 0{\cdot}02$	$P_{m1}\,(20) = 1$	$\theta_1 = 0{\cdot}9$	$\alpha_0 = 0{\cdot}01$	$P_{m0}\,(20) = 0{\cdot}8$	$\theta_0 = 0{\cdot}9$	$\rho_1 = 0{\cdot}9$	$\rho_2 = 0{\cdot}8$	σ^2
0·1	100	45·44	0·020	1·001	0·900	0·010	0·809	0·894	0·900	0·798	0·201
		(3·15)	(0·0008)	(0·027)	(0·020)	(0·0006)	(0·043)	(0·031)	(0·007)	(0·011)	(0·014)
0·1	400	46·08	0·020	1·001	0·901	0·010	0·803	0·897	0·900	0·799	0·201
		(1·26)	(0·0004)	(0·013)	(0·009)	(0·0003)	(0·019)	(0·014)	(0·003)	(0·006)	(0·007)
0·4	100	45·80	0·020	1·001	0·900	0·010	0·800	0·900	0·899	0·798	0·034
		(2·48)	(0·0003)	(0·013)	(0·009)	(0·0002)	(0·014)	(0·011)	(0·007)	(0·011)	(0·002)
0·4	400	46·02	0·020	1·000	0·900	0·010	0·800	0·899	0·900	0·800	0·034
		(1·15)	(0·0002)	(0·005)	(0·004)	(0·0001)	(0·008)	(0·006)	(0·003)	(0·006)	(0·001)

The location of the QTL is described by the map distance (in centimorgans) from the first marker of the linkage group (100 cM long). The hypothesized σ^2 value is 0·034 for $H^2 = 0{\cdot}4$ and 0·202 for $H^2 = 0{\cdot}1$.

Table 2. *The means of the MLEs of the QTL position and the parameters that model photosynthetic reaction norm processes for four different QTL genotypes* (*PpQq, Ppqq, ppQq and ppqq*) *at two hypothesized QTL P and Q and residual covariance matrices for 100 simulation replicates. The square roots of the mean squared errors of the MLEs are given in parentheses*

H^2	n	**P**	**Q**		PQ	Pq	pQ	pq	ρ_1	ρ_2	σ^2
True value		46	73	α	0·022	0·016	0·012	0·010	0·900	0·800	0·356
				P_m	1·350	0·850	0·660	0·350			
				θ	0·960	0·820	0·700	0·620			
0·1	100	44·32	72·60	α	0·022	0·016	0·012	0·010	0·900	0·798	2·124
		(5·19)	(6·23)		(0·002)	(0·099)	(0·006)	(0·005)	(0·010)	(0·011)	(0·163)
				P_m	1·362	0·927	0·732	0·373			
					(0·123)	(0·395)	(0·327)	(0·116)			
				$\hat{\theta}$	0·953	0·709	0·780	0·658			
					(0·039)	(0·322)	(0·353)	(0·342)			
0·1	400	45·84	73·28	α	0·022	0·017	0·013	0·010	0·900	0·800	2·135
		(3·04)	(5·25)		(0·001)	(0·005)	(0·008)	(0·003)	(0·003)	(0·006)	(0·078)
				P_m	1·349	0·880	0·645	0·356			
					(0·050)	(0·175)	(0·184)	(0·072)			
				$\hat{\theta}$	0·960	0·772	0·684	0·647			
					(0·012)	(0·231)	(0·305)	(0·283)			
0·4	100	47·36	70·48	α	0·022	0·016	0·012	0·010	0·900	0·798	0·355
		(6·36)	(6·42)		(0·001)	(0·004)	(0·003)	(0·003)	(0·006)	(0·0110)	(0·024)
				P_m	1·358	0·864	0·672	0·361			
					(0·039)	(0·139)	(0·171)	(0·051)			
				$\hat{\theta}$	0·964	0·750	0·733	0·590			
					(0·021)	(0·231)	(0·240)	(0·278)			
0·4	400	(47·44)	(71·08)	α	0·022	0·016	0·012	0·010	0·900	0·800	0·356
		(4·84)	(4·77)		(0·0004)	(0·002)	(0·002)	(0·002)	(0·003)	(0·006)	(0·012)
				P_m	1·351	0·854	0·658	0·354			
					(0·018)	(0·058)	(0·068)	(0·030)			
				$\hat{\theta}$	0·965	0·820	0·706	0·620			
					(0·016)	(0·101)	(0·117)	(0·110)			

or reaction norm has been increasingly studied by evolutionary and ecological biologists (Schlichting, 1986; Scheiner, 1993; Sultan, 2000, 2003*a*, *b*, 2004; Davidowitz & Nijhout, 2004). The genetic architecture of reaction norms in terms of the number of underlying quantitative trait loci and their actions/interactions can be unravelled by use of functional mapping (Wu & Lin, 2006), aimed at estimating and testing the degree and pattern of genetic regulation in shaping the phenotypic curves across ecological contexts. The construction of such an analytical model will help us to synthesize the information from genomics and developmental ecology and to gain an insight into the genomic basis of organismic

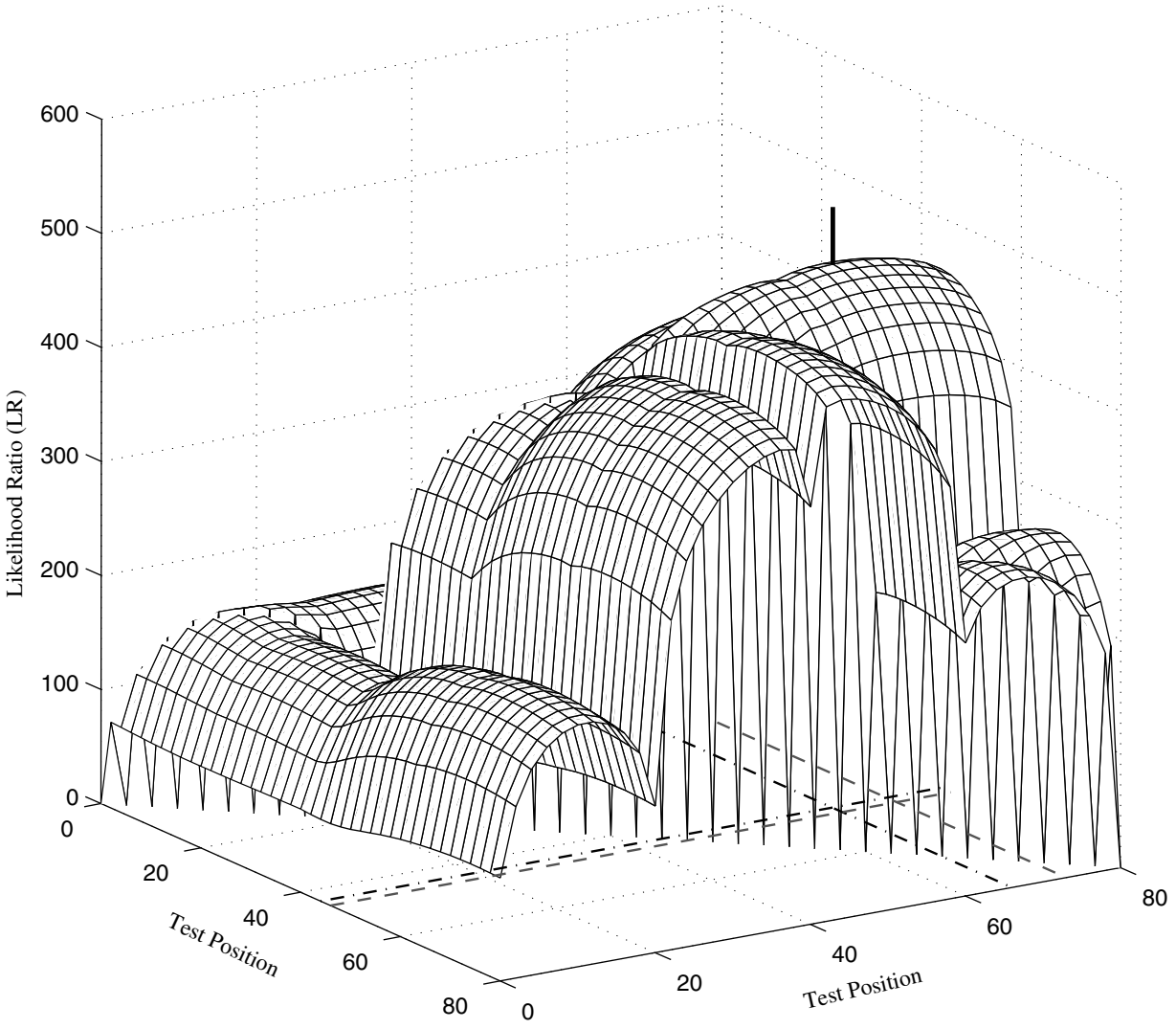

Fig. 3. Landscape of the log-likelihood ratios (LR) for testing the locations of two QTLs that control the reaction norm processes of photosynthetic rate to different irradiance and temperature levels. The red and black lines on the bottom surface indicate the true and estimated locations of the QTL, respectively.

responsiveness to changing environments (Dusheck, 2002; Sultan, 2005; Cronk, 2005).

In this article, we developed a functional-mapping-based model for testing the genetic control of multivariate reaction norms for an ecologically or physiologically significant trait. There is a pressing need for developing a general model for mapping the phenotype of reaction norms to multiple environmental factors. Many biological processes, such as the photosynthetic rate, can be modelled by a mathematical function that is derived from firm biologically principles (Thornely & Johnson, 1990; West *et al*., 2001). Other biological processes, such as thermal performance curves, can be modelled by a non-linear function that is derived by a best statistical fit to observational data (Kingsolver *et al*., 2004). While the slope of a parametric reaction norm measures the sensitivity of a genotype towards a change in the environment, the gradient of multivariate reaction norms defines the influence of interacting environmental factors on phenotypic values. In this sense, functional mapping, merged into models for ecological plasticity, can provide unique power to test fundamental issues of ecological and evolutionary roles of interactions between the genotype and environment in shaping phenotypic expression and evolution.

We have carried out simulation studies to investigate the statistical behaviour of our functional mapping used to study the genetic basis of reaction norms. It has been found that the model performs well in terms of the estimation accuracy, precision and robustness. Some of the good features of the model result from elegant expressions of the structured non-genetic residual covariance matrix by commonly used time series processes (Diggle *et al*., 2002; Zimmerman & Núñez-Antón, 2001). For example, closed forms exist for the determinant and inverse of the structured

covariance matrix when it is modelled by an autoregressive (AR) or antedependence (SAD) process. Zhao *et al*. (2005*a*) showed that both AR and SAD can be interesting alternatives, although SAD can be more general than AR under some circumstances. For many practical problems, non-genetic effects can be dissolved into autocorrelated permanent environmental and uncorrelated random residual effects (Ptak & Schaeffer, 1993; Lund *et al*., 2002; Kolmodin *et al*., 2002), with a new parameter used to define the ratio of the variances due to these two effects. The AR or SAD processes have been shown to be powerful for modelling the structure of the permanent environmental covariance (J. Wu and R. L. Wu, unpublished results).

In modelling reaction norms to multiple environmental factors, a so-called completely separable structure has been used to facilitate computation, but it does not take into account the interactions between the two different reaction norm processes. A model for non-separable isotropic spatio-temporal variograms could be built to characterize the dependence between the two random variables (Porcu *et al*., 2006*a*, *b*) with copulas, a technique widely used in the financial context (Nelsen, 1999), and by extending Sklar's and Nelsen's theorems to isotropic spatio-temporal random fields. The advantage of this approach is that the marginal reaction norm process dependence can be modelled separately and the interaction between different environments is achieved through an appropriate choice of a parametric copula. Using the Archimedean copula as a generating class, a proper generating function can be chosen to reflect the interaction between different environments.

In theory, our general framework for eco-devo functional mapping can be extended to higher dimensions. The significance of higher dimensions can be exemplified by a photosynthetic rate process. In our example, photosynthetic rate is assumed to be controlled by irradiance and temperature (Thornley & Johnson, 1990; Wu, 1993). However, other environmental factors such as concentration, leaf age and nutrient contents also play an important role in regulating photosynthetic rate and, thus, the joint inclusion of such factors should provide a better insight into the genetic basis of this physiological process. Although this will present a statistical challenge, further modelling and analysis are worthwhile using the recent advances in statistics in the field. For example, the procedure for mapping multivariate developmental trajectories by Zhao *et al*. (2005*b*) can be used to construct the theory for the functional mapping of reaction norms for multiple traits to multiple environmental factors.

Many biological processes can be mathematically described, but there are many others for which a rigorous mathematical function cannot be defined. For such processes it might be difficult to perform a parametric analysis. However, for those reaction norm processes for which parametric functions do not exist, a random regression model for approximating the mean structure of longitudinal data should be used (see Kolmodin *et al*., 2002). Lin & Wu (2006) used Legendre polynomials to model curves that cannot be fitted by mathematical equations. Alternatively, an approach based on B-spline basis functions, which has been well developed in the statistical literature (Rice & Wu, 2001), can be used for non-parametric regression fitting. The B-spline approach constructs curves from pieces of lower degree polynomials smoothed at selected pointed (knots). Brown *et al*. (2005) extended the B-spline basis to model multiple longitudinal variables. The idea of B-spline curve fitting will be incorporated into the functional mapping model, with the aim of increasing the breadth of the use of functional mapping in solving practical genetic problems.

We thank the two anonymous referees for constructive comments on the earlier version of this manuscript. This work is partially supported by grants (09-95671 and 30230300) from the National Natural Science Foundation of China and from NSF (0540745).

Appendix

Below, we describe a mathematical procedure for calculating the integrals and derivatives of the photosynthetic reaction norm curves used to construct hypotheses (6)–(12).

$$\int P(s_1,s_2)ds_1 = \frac{1}{4\theta}\left(s_1^2\alpha + \frac{2(T^*-s_2)s_1\alpha p_m(20)+[(20-T^*)s_1\alpha+(T^*-s_2)(2\theta-1)p_m(20)]K}{(T^*-20)\alpha} + \frac{4(T^*-s_2)^2(\theta-1)\theta\log\{2[(s_2-T^*)(2\theta-1)p_m(20)+(T^*-20)(s_1\alpha+K)]\}p_m^2(20)}{(T^*-20)^2\alpha}\right),$$

$$\int P(s_1,s_2)ds_2 = \frac{1}{2\theta}\left(s_2s_1\alpha + \frac{2T^*s_2p_m(20)-s_2^2p_m(20)}{2(T^*-20)} + \frac{[(20-T^*)s_1\alpha(2\theta-1)+(T^*-s_2)p_m(20)]K}{2p_m(20)} + \frac{2(T^*-20)s_1^2\alpha^2(\theta-1)\theta\log\{2[(s_2-T^*)p_m(20)+(T^*-20)(s_1\alpha(2\theta-1)+K)]\}}{p_m(20)}\right)$$

$$\iint P(s_1,s_2)ds_2ds_1 = \frac{1}{2\theta}\left(\frac{1}{2}s_2s_1^2\alpha - \frac{2(T^*-20)s_1^3\alpha^2(\theta-1)\theta}{9p_m(20)} + \frac{1}{3p_m(20)}(2(T^*-20)s_1^3\alpha^2(\theta-1)\theta\log[2((s_2-T^*)p_m(20) + (T^*-20)((s_1\alpha(2\theta-1)+K)]\right) + \frac{T^*s_2s_1p_m(20)}{T^*-20} + \frac{s_2^2s_1p_m(20)}{40-2T^*} + \frac{1}{(T^*-20)^2\alpha}\left(4(T^*-s_2)^3(\theta-1)^2\theta^2 \log[2(-20s_1\alpha + T^*s_1\alpha + T^*p_m(20) - s_2p_m(20) - 2T^*\theta p_m(20) + 2s_2\theta p_m(20) + (T^*-20)K)]p_m^2(20) - \frac{1}{3(T^*-20)^2\alpha}(2(T^*-s_2)^3(\theta-1)\theta(1-6\theta+6\theta^2)) \log[2(-20s_1\alpha + T^*s_1\alpha + T^*p_m20 - s_2p_m(20) - 2T^*\theta p_m(20) + 2s_2\theta p_m(20)(T^*-20)K)]p_m^2(20)) - \frac{1}{3(T^*-20)\alpha}((T^*-s_2)(\theta-1)\theta((T^*-20)s_1\alpha + 3(T^*-s_2)(2\theta-1)p_m(20))K) + \frac{K}{6p_m(20)}\left[(20-T^*)s_1^2\alpha(1-2\theta) + 2(T^*-s_2)s_1\left(1-\theta+\theta^2\right)p_m(20) + \frac{(T^*-s_2)^2(1+4\theta-18\theta^2+12\theta^3)p_m^2(20)}{(T^*-20)\alpha}\right]$$

where

$$K = \sqrt{s_1^2\alpha^2 + \frac{(T^*-s_2)p_m(20)(2(20-T^*)s_1\alpha(2\theta-1)+(T^*-s_2)p_m(20))}{(T^*-20)^2}}.$$

$$\frac{\partial}{\partial s_1}P(s_1,s_2) = \frac{1}{2\theta}\left\{\alpha + \frac{\alpha((20-T^*)s_1\alpha + (T^*-s_2)(2\theta-1)p_m(20))}{(T^*-20)\sqrt{\frac{4(T^*-s_2)s_1\alpha\theta p_m(20)}{20-T^*} + \left(s_1\alpha + \frac{(T^*-s_2)p_m(20)}{T^*-20}\right)^2}}\right\}$$

$$\frac{\partial}{\partial s_2}P(s_1,s_2) = \frac{1}{2\theta}\left\{p_m(20)\left(\frac{1}{20-T^*} + \frac{(20-T^*)s_1\alpha(2\theta-1)+(T^*-s_2)p_m(20)}{(T^*-20)^2\sqrt{\frac{4(T^*-s_2)s_1\alpha\theta p_m(20)}{20-T^*} + \left(s_1\alpha + \frac{(T^*-s_2)p_m(20)}{T^*-20}\right)^2}}\right)\right\}$$

$$\frac{\partial}{\partial s_1 s_2}P(s_1,s_2) = \left(2(T^*-s_2)s_1\alpha^2(\theta-1)p_m(20)^2\right) \times\left((T^*-20)^2s_1^2\alpha^2 + (T^*-s_2)p_m(20)(2(20-T^*)s_1\alpha(2\theta-1)+(T^*-s_2)p_m(20))\right)^{-1} \times\left(\sqrt{\frac{4(T^*-s_2)s_1\alpha\theta p_m(20)}{20-T^*} + \left(s_1\alpha + \frac{(T^*-s_2)p_m(20)}{T^*-20}\right)^2}\right)^{-1}$$

References

Arthur, W. (2002). The emerging conceptual framework of evolutionary developmental biology. *Nature* **415**, 757–764.

Borlak, J. (2005). *Handbook of Toxicogenomics: Strategies and Applications*. New York: Wiley.

Brown, E. B., Ibrahim, J. G. & DeGruttola, V. (2005). A flexible B-spline model for multiple longitudinal biomarkers and survival. *Biometrics* **61**, 64–73.

Cronk, Q. (2005). Plant eco-devo: the potential of poplar as a model. *New Phytologist* **166**, 39–48.

Davidowitz, G., D'Amico, L. J. & Nijhout, H. F. (2003). Critical weight in the development of insect body size. *Evolution & Development* **5**, 188–197.

Davidowitz, G., D'Amico, L. J. & Nijhout, H. F. (2004). The effects of enviornmental variation on a mechanism that controls insect body size. *Evolutionary Ecology Research* **6**, 49–62.

Davidowitz, G. & Nijhout, H. F. (2004). The physiological basis of reaction norms: the interaction between growth rate, the duration of growth and body size. *Integrative and Comparative Biology* **44**, 443–449.

Diggle, P. J., Heagerty, P., Liang, K. Y. & Zeger, S. L. (2002). *Analysis of Longitudinal Data*. Oxford: Oxford University Press.

Dusheck, J. (2002). It's the ecology, stupid! *Nature* **418**, 578–579.

Gabriel, K. R. (1962). Ante-dependence analysis of an ordered set of variables. *Annals of Mathematics and Statistics* **33**, 201–212.

Gomulkiewicz, R. & Kirkpatrick, M. (1992). Quantitative genetics and the evolution of reaction norms. *Evolution* **46**, 390–311.

Jiang, C. & Zeng, Z.-B. (1995). Multiple trait analysis of genetic mapping for quantitative trait loci. *Genetics* **140**, 1111–1127.

Kingsolver, J. G., Ragland, G. J. & Shlicht, J. G. (2004). Quantitative genetics of continuous reaction norms: thermal sensitivity of caterpillar growth rates. *Evolution* **58**, 1521–1529.

Kirkpatrick, M. & Heckman, N. (1989). A quantitative genetic model for growth, shape, reaction norms, and other infinite-dimensional characters. *Journal of Mathematical Biology* **27**, 429–450.

Kolmodin, R., Strandberg, E., Madsen, P., Jensen, J. & Jorjani, H. (2002). Genotype by environment interaction in Nordic dairy cattle studied by use of reaction norms. *Acta Agriculturæ Scandinavica Section A* **52**, 11–24.

Lander, E. S. & Botstein, D. (1989). Mapping Mendelian factors underlying quantitative traits using RFLP linkage maps. *Genetics* **121**, 185–199.

Lin, M. & Wu, R. L. (2006). A joint model for nonparametric functional mapping of longitudinal trajectories and time-to-events. *BMC Bioinformatics* **15**, 138.

Lund, M. S., Sorensen, A. C. & Madsen, P. (2002). Linkage analysis in longitudinal data using random regression. *Proceedings of the 7th World Congress on Genetics Applied to Livestock Production. CD-ROM communication no*. 21–28.

Lynch, M. & Walsh, B. (1998). *Genetics and Analysis of Quantitative Traits*. Sunderland, MA: Sinauer.

Ma, C.-X., Casella, G. & Wu, R. L. (2002). Functional mapping of quantitative trait loci underlying the character process: a theoretical framework. *Genetics* **161**, 1751–1762.

Nelsen, R. B. (1999). *An Introduction to Copulas*. New York: Springer.

Núñez-Antón, V., Rodriguez-Poo, J. M. & Vieu, P. (1999). Longitudinal data with nonstationary errors: a nonparametric three-stage approach. *Test* **8**, 201–231.

Pan, J. X. & Mackenzie, G. (2003). On modelling mean-covariance structures in longitudinal studies. *Biometrika* **90**, 239–244.

Porcu, E., Gregori, P. & Mateu, J. (2006). Nonseparable stationary anisotropic space/time covariance functions. *Stochastic Environmental Research and Risk Assessment* **21**, 113–122.

Porcu, E., Mateu, J., Zini, A. & Pini, R. (2007). Modelling spatio-temporal data: A new variogram and covariance structure proposal. *Statistics & Probability Letters* **77**, 83–89.

Pourahmadi, M. (1999). Joint mean-covariance models with applications to longitudinal data: Unconstrained parameterisation. *Biometrika* **86**, 677–690.

Ptak, E. & Schaeffer, L. R. (1993). Use of test-day yields for genetic evaluation of dairy sires and cows. *Livestock Production Science* **34**, 23–34.

Raff, R. A. (2000). Evo-devo: the evolution of a new discipline. *Nature Reviews Genetics* **1**, 74–79.

Rice, J. A. & Wu, C. O. (2001). Nonparametric mixed effects models for unequally sampled noisy curves. *Biometrics* **57**, 253–259.

Rice, S. H. (2002). A general population genetic theory for the evolution of developmental interactions. *Proceedings of the National Academy of Sciences of the USA* **99**, 15518–15523.

Richards, F. J. (1959). A flexible growth function for empirical use. *Journal of Experimental Botany* **10**, 290–300.

Scheiner, S. M. (1993). Genetics and evolution of phenotypic plasticity. *Annual Review of Ecology and Systematics* **24**, 35–68.

Schlichting, C. D. (1986). The evolution of phenotypic plasticity in plants. *Annual Review of Ecology and Systematics* **17**, 667–693.

Schlichting, C. D. & Pigliucci, M. (1998). *Phenotypic Evolution: A Reaction Norm Perspective*. Sunderland, MA: Sinauer.

Stearns, S. C. (1989). The evolutionary significance of phenotypic plasticity. *BioScience* **39**, 436–445.

Sultan, S. E. (2000). Phenotypic plasticity for plant development, function and life-history. *Trends in Plant Science* **5**, 537–542.

Sultan, S. E. (2003*a*). The promise of ecological developmental biology. *Journal of Experimental Zoology* **296B**, 1–7.

Sultan, S. E. (2003*b*). Phenotypic plasticity in plants: a case study in ecological development. *Evolution and Development* **5**, 25–33.

Sultan, S. E. (2004). Promising research directions in plant phenotypic plasticity. *Perspectives in Plant Ecology, Evolution and Systematics* **6**, 227–333.

Sultan, S. E. (2005). An emerging focus on plant ecological development. *New Phytologist* **166**, 1–5.

Thornley, J. H. M. & Johnson, I. R. (1990). *Plant and Crop Modelling: A Mathematical Approach to Plant and Crop Physiology*. Oxford: Clarendon Press.

Via, S., Gomulkiewicz, R., de Jong, G., Scheiner, S. E., Schlichting, C. D. & van Tienderen, P. (1995). Adaptive phenotypic plasticity: consensus and controversy. *Trends in Ecology and Evolution* **10**, 212–217.

von Bertalanffy, L. (1957). Quantitative laws in metabolism and growth. *Quarterly Review of Biology* **32**, 217–231.

West, G. B., Brown, J. H. & Enquist, B. J. (2001). A general model for ontogenetic growth. *Nature* **413**, 628–631.

Wolf, J. B. (2002). The geometry of phenotypic evolution in developmental hyperspace. *Proceedings of the National Academy of Sciences of the USA* **99**, 15849–15851.

Wu, R. L. (1993). Simulated optimal structure of a photosynthetic system: Implications for the breeding of forest crop ideotype. *Canadian Journal of Forest Research* **23**, 1631–1638.

Wu, R. L. (1998). The detection of plasticity genes in heterogeneous environments. *Evolution* **54**, 967–977.

Wu, R. L. & Lin, M. (2006). Functional mapping: how to map and study the genetic architecture of dynamic complex traits. *Nature Reviews Genetics* **7**, 229–237.

Wu, R. L., Ma, C.-X., Lou Y.-X. & Casella, G. (2003*a*). Molecular dissection of allometry, ontogeny and plasticity: A genomic view of developmental biology. *BioScience* **53**, 1041–1047.

Wu, R. L., Ma, C.-X., Zhao, W. & Casella, G. (2003*b*). Functional mapping of quantitative trait loci underlying

growth rates: A parametric model. *Physiological Genomics* **14**, 241–249.

Wu, R. L., Ma, C.-X., Lin, M. & Casella, G. (2004*a*). A general framework for analyzing the genetic architecture of developmental characteristics. *Genetics* **166**, 1541–1551.

Wu, R. L., Ma, C.-X., Lin, M., Wang, Z. H. & Casella, G. (2004*b*). Functional mapping of growth QTL using a transform-both-sides logistic model. *Biometrics* **60**, 729–738.

Wu, R. L., Wang, Z. H., Zhao, W. & Cheverud, J. M. (2004*c*). A mechanistic model for genetic machinery of ontogenetic growth. *Genetics* **168**, 2383–2394.

Wu, W. B. & Pourahmadi, M. (2003). Nonparametric estimation of large covariance matrices of longitudinal data. *Biometrika* **90**, 831–844.

Zhao, W., Wu, R. L., Ma, C.-X. & Casella, G. (2004). A fast algorithm for functional mapping of complex traits. *Genetics* **167**, 2133–2137.

Zhao, W., Chen, Y. Q., Casella, G., Cheverud, J. M. & Wu, R. L. (2005*a*). A non-stationary model for functional mapping of longitudinal quantitative traits. *Bioinformatics* **21**, 2469–2477.

Zhao, W., Hou, W., Littell, R. C. & Wu, R. L. (2005*b*). Structured antedependence models for functional mapping of multivariate longitudinal quantitative traits. *Statistical Methods in Molecular Genetics and Biology* **4**, http://www.bepress.com/sagmb/vol4/iss1/art33/

Zimmerman, D. L. & Núñez-Antón, V. (2001). Parametric modeling of growth curve data: An overview (with discussion). *Test* **10**, 1–73.